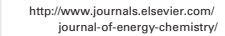


Contents lists available at ScienceDirect

# Journal of Energy Chemistry



journal homepage: www.elsevier.com/locate/jechem

# Communication

# Towards an all-vanadium redox flow battery with higher theoretical volumetric capacities by utilizing the $VO^{2+}/V^{3+}$ couple

Wentao Duan, Bin Li, Dongping Lu, Xiaoliang Wei, Zimin Nie, Vijayakumar Murugesan, James P. Kizewski, Aaron Hollas, David Reed, Vincent Sprenkle, Wei Wang\*

Pacific Northwest National Laboratory, P.O. Box 999, Richland, Washington 99352, United States

#### ARTICLE INFO

Article history:
Received 9 January 2018
Revised 24 April 2018
Accepted 24 May 2018
Available online 15 June 2018

Keywords: Vanadium Redox reactions Redox flow battery Energy density Cu

#### ABSTRACT

An all-vanadium redox flow battery with V(IV) as the sole parent active species is developed by accessing the  $VO^{2+}/V^{3+}$  redox couple. These batteries, referred to as V4RBs, possess a higher theoretical volumetric capacity than traditional VRBs. Copper ions were identified as an effective additive to boost the battery performance.

© 2018 Published by Elsevier B.V. and Science Press on behalf of Science Press and Dalian Institute of Chemical Physics, Chinese Academy of Sciences

With increasing demands on renewable energy deployments and electric grid modernizations, redox flow batteries (RFBs) have recently attracted a great wealth of research interests [1–3]. All-vanadium redox flow batteries (VRBs), first invented by the Skyllas-Kazacos group [4], are perhaps the most well-developed and promising RFB system, and have already been deployed at large scale [5,6]. Tremendous research efforts have been invested towards further developments of the system. For example, by optimizing the electrolyte solution chemistry, the energy density in VRBs can be improved by a 70% margin, together with a 80% increase in temperature range of stable operation [7].

In VRBs, four different oxidation states of the same element are employed: V (V, IV, III, and II). As shown in Fig. 1, in strong acids, the corresponding species of these oxidation states constitute three redox couples with a single electron transfer:  $VO_2^+/VO^{2+}$ ,  $VO^{2+}/VO^{3+}$  and  $VO^{3+}/VO^{2+}$ . Conventional VRBs utilize the  $VO_2^+/VO^{2+}$  and  $VO^{3+}/VO^{2+}$  couples to undergo the following electrochemical reactions, and have a theoretical cell voltage of 1.25 V:

$$\begin{split} & \text{Cathode half} - \text{cell}: VO_2^+ + 2H^+ + e^- \overset{Discharge}{\overset{Charge}{\longleftrightarrow}} H_2O + VO^{2+} \\ & \text{Anode half} - \text{cell}: V^{2+} \overset{Discharge}{\overset{Discharge}{\longleftrightarrow}} V^{3+} + e^- \end{split}$$

E-mail address: wei.wang@pnnl.gov (W. Wang).

Overall : 
$$VO_2^+ + V^{2+} + 2H^+ \overset{Discharge}{\longleftrightarrow} V^{3+} + VO^{2+} + H_2O$$

In traditional VRB systems, the VO<sup>2+</sup>/V<sup>3+</sup> redox couple is not utilized as the energy-bearing active materials. Although it often plays an important role in the balancing step of VRBs for bench-top flow cell tests, the  $VO^{2+}/V^{3+}$  redox reaction is often considered a self-discharge reaction after crossover [8,9]. As shown in Fig. 1, the reaction between VO<sub>2</sub>+/VO<sup>2+</sup> and VO<sup>2+</sup>/V<sup>3+</sup> couples is favourable thermodynamically, with a theoretical cell voltage of 0.66 V. This reaction can be coupled with the reaction in conventional VRBs to produce a VRB, namely V4RB, which utilizes the same parent active species (VO2+) on both sides of the flow battery. With a catholyte:anolyte volume ratio of 2:1, VO<sup>2+</sup> is converted to VO<sub>2</sub>+ and V<sup>2+</sup> at positive and negative sides, respectively. Such designs will further expand the merits of VRBs by improving the utilization of vanadium ions, and hence enhancing the theoretical volumetric capacity. Furthermore, the employment of the same parent active materials (i.e. V(IV)) could alleviate the crossover concerns at the discharged state, and potentially simplify the rebalancing step as

The feasibility of V4RBs was first demonstrated with an electrolyte composition of  $2\,M$  VOSO<sub>4</sub> in  $5\,M$  HCl solutions (denoted as V225), and a catholyte:anolyte volume ratio of 2:1. At a current density of  $50\,mA/cm^2$ , two major sets of charge/discharge plateaus were observed from voltage profiles of the flow cell (Fig. 2a). These two sets presumably correspond to the two-step reactions of the

<sup>\*</sup> Corresponding author.

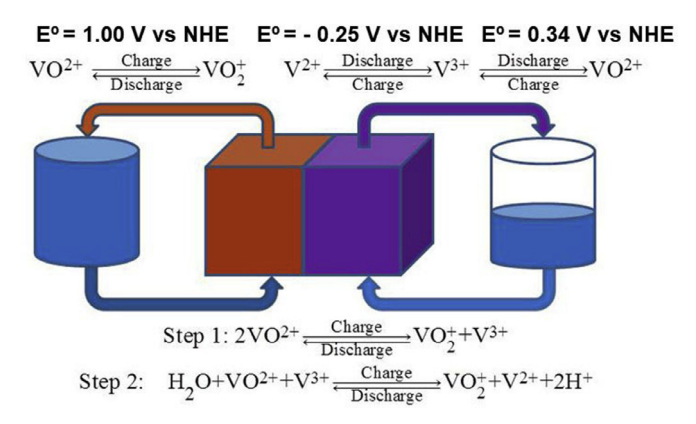
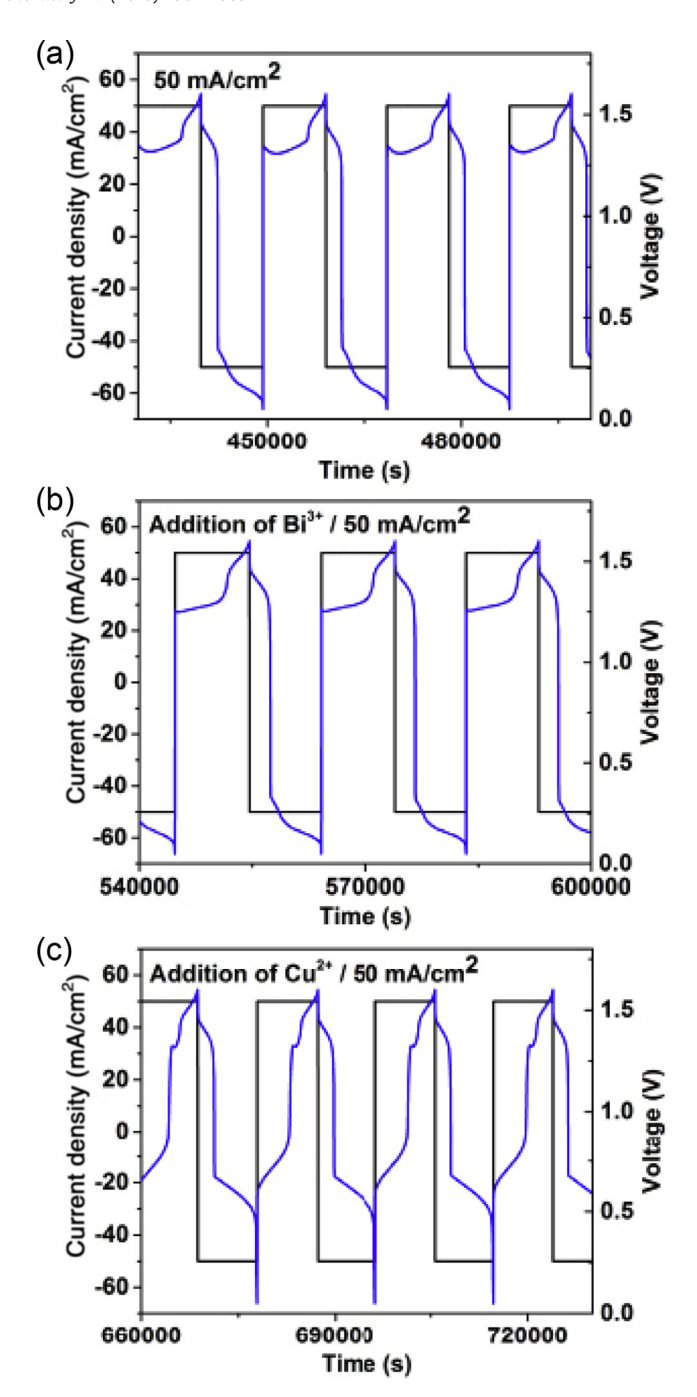


Fig. 1. Schematic figure for the design of all-vanadium (IV) flow batteries, or V4RB, with the same parent active species  $(V0^{2+})$ .

 ${\rm VO_2}^+/{\rm VO^{2+}}$  couple vs  ${\rm VO^{2+}/V^{3+}}$  and  ${\rm V^{3+}/V^{2+}}$  couples, as shown in Fig. 1.

As for the cycling performance, the round-trip coulombic efficiency (CE) was around 97%, while the energy efficiency (EE) was only around 35% at a current density of 50 mA/cm<sup>2</sup> (Fig. S1 in the Supplementary Information). This low energy efficiency is due to the high over-potentials during Step 1, as indicated by the large gaps between charging and discharging plateaus in Fig. 2(a). Polarizations in VRBs are mostly attributed to Ohmic loss, mass transfer resistance, and charge transfer barrier [11]. With similar environments, Step 1 and 2 shared comparable Ohmic and concentration polarizations. Therefore, their substantial variations in over-potentials originate from intrinsic differences in kinetics of  $VO^{2+}/V^{3+}$  and  $V^{3+}/V^{2+}$  couples at electrode surfaces. In fact, previous voltammetry studies suggest that the VO<sup>2+</sup>/V<sup>3+</sup> couple demands a large activation energy during electrochemical reactions [8]. By decreasing the over-potential with a lower current density (20 mA/cm<sup>2</sup>), EE can be promoted to around 50%. It is interesting to notice that a third discharge plateau was observed in the voltage profile at 20 mA/cm<sup>2</sup> (Fig. S2 in the Supplementary Information), indicating a possibly more complex process.

To enhance the performance of this V4RB system demands improvements on the kinetics of charge transfer processes in Step 1, especially the  $VO^{2+}/V^{3+}$  couple. Inspired by the fact that bismuth [11] and copper [12] nanoparticles are effective catalysts in conventional VRBs towards the  $V^{3+}/V^{2+}$  couple, two metal salts in the form of BiCl<sub>2</sub> and CuCl<sub>2</sub> were sequentially added to the anolyte side of the above flow cell system to test their effects on cell performances. Voltage profiles after the addition of Bi and Cu ions are illustrated in Fig. 2(b, c). The introduction of these ions led to a slight decline of CE, but nevertheless promoted VEs and EEs (Fig. S1), although by a different margin. Specifically, compared with Bi ions, Cu ions are more effective in boosting the performance of this V4RB, and EEs rose to above 70% with their presence. Indeed, as shown in Fig. 2(b) and Fig. S3, the addition of Bi ions has minimal effect on the voltage curves of Step 1 (i.e. conversions related to the  $VO^{2+}/V^{3+}$  couple). The first charging plateau was lowered by a small margin (around 0.04 to 0.05 V), while the second discharging plateau almost overlapped with that of pristine electrolytes (V225). This suggests that deposited Bi metals during charging, instead of Bi ions, might be contributing. The mechanism might be by either lowering Ohmic losses through better electrode conductivities, or suppressing charge transfer polarizations through possible catalytic effects towards the VO<sup>2+</sup>/V<sup>3+</sup> couple. In comparison, Cu ions drastically altered the voltage profiles of Step 1, and significantly reduced the over-potentials. Two distinct charging plateaus were observed for Step 1 (Fig. 2c and Fig. S3 in the Supporting In-



**Fig. 2.** Voltage profiles of the V4RB at a current density of 50 mA/cm<sup>2</sup> before and after the addition of metal salts: a: before salt additions, b: after the addition of 0.2 mmol BiCl<sub>3</sub> (apparent concentration: 10 mM) to the anolyte side, and c: after further addition of 0.2 mmol CuCl<sub>2</sub> (apparent concentration: 10 mM) to the anolyte side.

formation), and compared with that before Cu addition, the first plateau was about 0.5 to 0.6 V lower, while the second one was on a similar voltage level. The two charging plateaus, however, correspond to only one discharging plateau, which was increased by about 0.4 V after the addition of Cu. Such phenomena suggest that Cu ions or their derivative species during cycling only function within a certain SOC range during charging of Step 1. In the electrochemical processes during cycling, cyclic voltammetry (CV) results of the V225 electrolyte with 10 mM BiCl<sub>3</sub> and 10 mM CuCl<sub>2</sub> reveal a pair of peaks near 0.3 V vs. AgCl/Ag (Fig. 3a). This pair of peaks is around 0.6 to 0.7 V lower than that of the VO<sub>2</sub>+/VO<sup>2+</sup>

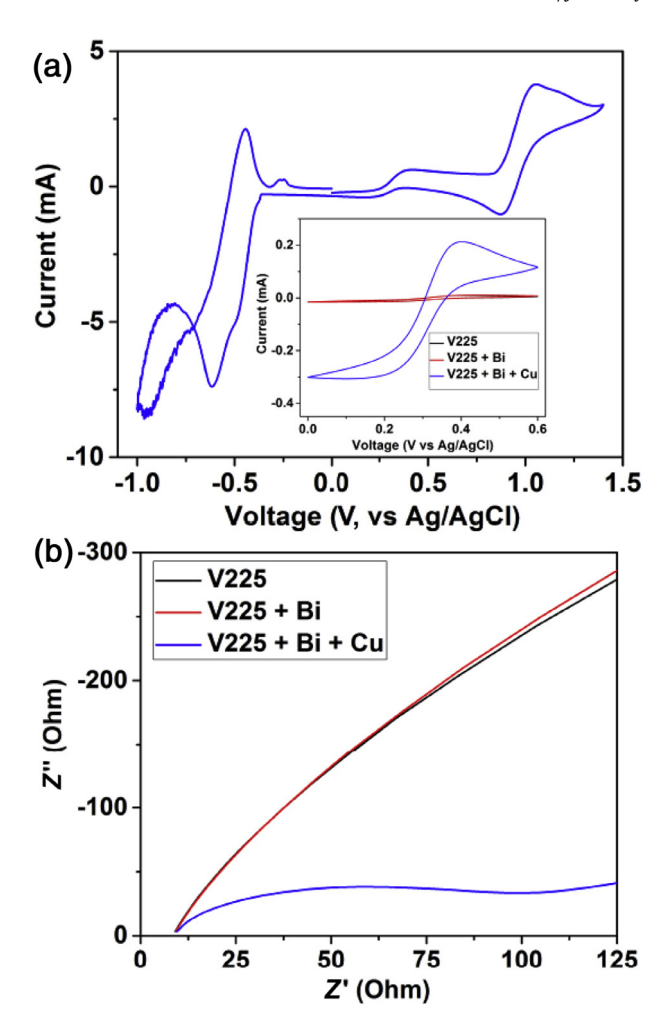


**Fig. 3.** (a) CV results of the  $2\,M$  VOSO<sub>4</sub>- $5\,M$  HCl electrolyte with the addition of  $10\,mM$  BiCl<sub>3</sub> and  $10\,mM$  CuCl<sub>2</sub>. Inset: Comparison of CV results before and after addition of metal salts. (b) Impedance analysis of the  $2\,M$  VOSO<sub>4</sub>- $5\,M$  HCl electrolyte before and after the addition of  $10\,mM$  BiCl<sub>3</sub> and  $10\,mM$  CuCl<sub>2</sub>. The scan rate of CV was  $10\,mV/s$ , and the impedance analysis was conducted at  $0.3\,V$  vs. the AgCl/Ag reference electrode.

couple. The value of such a potential gap correlates well with those of the first charging plateau and the discharging plateau for Step 1, indicating that the process corresponding to these peaks is responsible for the enhancement of battery performances. The impact of Cu species on this pair of peaks is cross-validated by both CV and electrochemical impedance spectroscopy results (Fig. 3 and Fig. S4). The exact process during cycling and mechanism for performance improvements are still under investigation. With high concentrations of chloride ions in the electrolytes, the preliminary assumption is that Cu(I) species [13,14] are playing an important role in the process. These species either catalyze the electrochemical reactions of the  $VO^{2+}/V^{3+}$  couple, or work as electron-transfer mediators. At higher SOC range of Step 1, however, these species are further reduced to Cu metals, and lose their functions. As a result, the over-potential returned to the level observed in the absence of Cu ions, which explains the splitting of charging plateaus for Step 1 discussed above.

To confirm the role of Cu additives on the cell performance solely for Step 1, a symmetric V4RB system was designed with V(IV) as the only parent active material, and a volume ratio of 1:1 for the catholyte and anolyte (Fig. 4a). In this cell,  $VO^{2+}$  is converted to  $VO_2^+$  and  $V^{3+}$  at positive and negative sides, respectively. Without Cu additives, significant over-potentials were ob-

served at various current densities from 50 – 100 mA/cm² (Fig. S5). The addition of Cu ions, however, significantly lowered the overpotentials, and with a voltage cut-off at 0.9 V (Fig. 4b), the symmetric V4RB cell had an average CE of 98%, VE of 79% and EE of 77% at a current density of 50 mA/cm². The highest volumetric capacity was around 18 Ah/L, (Fig. 4c). Higher current densities led to a slight increase of CEs by suppressing crossover and self-discharge (Fig. 4c), but resulted in a significant decline in EEs with enlarged over-potentials, as indicated from the change of voltage profiles in Fig. 4b. It is noteworthy that VEs kept increasing in the initial cycles, which correlates with the fact that over-potentials were decreasing over initial cycles (Fig. S6), suggesting the existence of an activation period. The activation process is probably associated with the formation and enrichment of Cu (I) species near electrode surfaces.

After confirming the effect of Cu additives on the reaction in Step 1, performances of V4RB cells (catholyte:anolyte volume being 2:1) were then evaluated with CuCl<sub>2</sub> as the sole additive to anolyte sides, and results are as shown in Fig. 5. With a voltage cut-off at 1.6 V (Fig. 5a), the peak volumetric discharge capacity was around 28.0 Ah/L at a current density of 50 mA/cm<sup>2</sup>. Such a capacity output is only ~80% of the theoretical value (35.6 Ah/L) due to the limited voltage cut-off, but is nonetheless higher than the theoretical value (26.8 Ah/L) of conventional VRBs with the same concentration of vanadium species. Mean values of CE, VE and EE were 96%, 81% and 78% at the current density of 50 mA/cm<sup>2</sup>, respectively (Fig. 5b). During cell cycling, an activation period also existed in the initial cycles (Fig. S7a) with VE increasing over time, while a slight decline of VE was observed in later cycles. The decline of VE correlates with the change of capacity ratios between Step 1 and Step 2. As shown in Fig. S7b, the capacity percentile contributed by Step 1, which corresponds to lower VEs than Step 2, was increasing over cycles. These changes probably originated from a combination of crossover related concentration shift and side reactions such as gas evolutions, which also led to capacity decay. Capacity remediation techniques [9,15] such as remixing and periodic volume transfer are currently under investigation. The prerequisite of these techniques is that the presence of Cu ions in the catholyte side cannot be detrimental to the cell performance. Indeed, as shown in Fig. S8, the performance of a V4RB cell with 10 mM CuCl<sub>2</sub> on both catholyte and anolyte sides is comparable to that with  $10\,\mathrm{mM}$  CuCl $_2$  only on the anolyte

To conclude, by accessing the  $VO^{2+}/V^{3+}$  couple, herein we presented the design of a VRB system that utilizes the same parent active species ( $VO^{2+}$ ) on both sides of the flow battery. Cu ions were identified as an effective additive to boost the performance of this V4RB system, and higher volumetric capacity outputs were achieved with better vanadium utilizations. The exact mechanism for the enhancements with Cu additives is currently under investigation, but Cu(I) species were likely involved in the charge transfer process of  $VO^{2+}/V^{3+}$  redox reaction. Besides employing electrolyte additives, electrode modifications with catalysts such as Ir [16] or carbon nanotubes [17] might also be viable to facilitate the kinetics of the  $VO^{2+}/V^{3+}$  couple, as indicated in previous cyclic voltammetry studies. Such possibilities are being explored to further boost performances of the new VRB design.

# Acknowledgments

The authors would like to acknowledge financial support from the U.S. Department of Energy's (DOE) Office of Electricity Delivery and Energy Reliability (OE) under contract number 57558. Pacific Northwest National Laboratory is a multi-program national

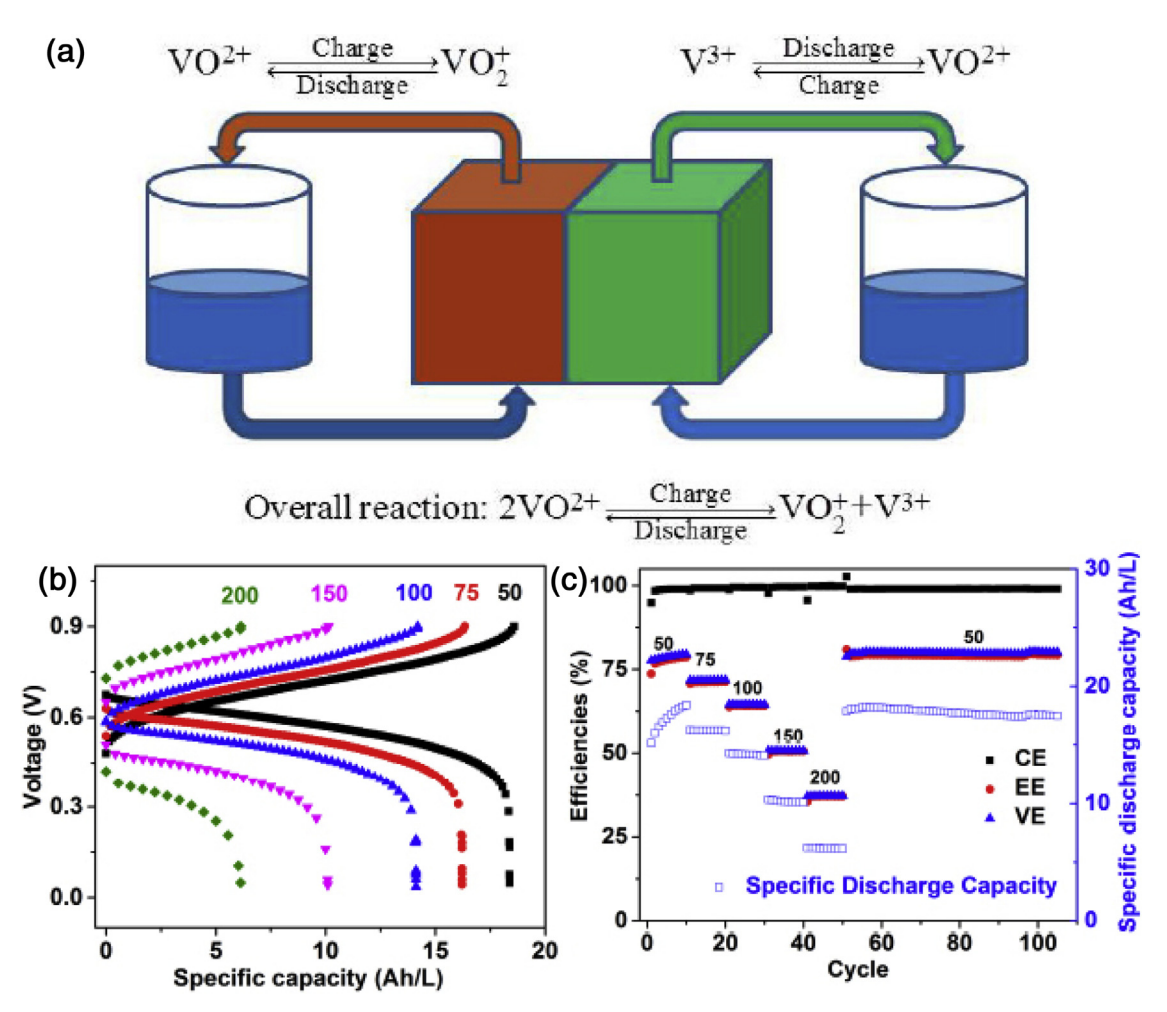


Fig. 4. Schematic figure (a) and cycling performances of the symmetric V4RB cell with 10 mM CuCl<sub>2</sub> at the anolyte side: (b) voltage profiles at different current densities and (c) cell efficiencies and specific discharge capacities. Numbers above each voltage or efficiency plot indicate corresponding current densities with units of mA/cm<sup>2</sup>. Voltage curves in (b) are from Cycle 10, 20, 30, 40 and 50. The theoretical volumetric capacity is 26.8 Ah/L.

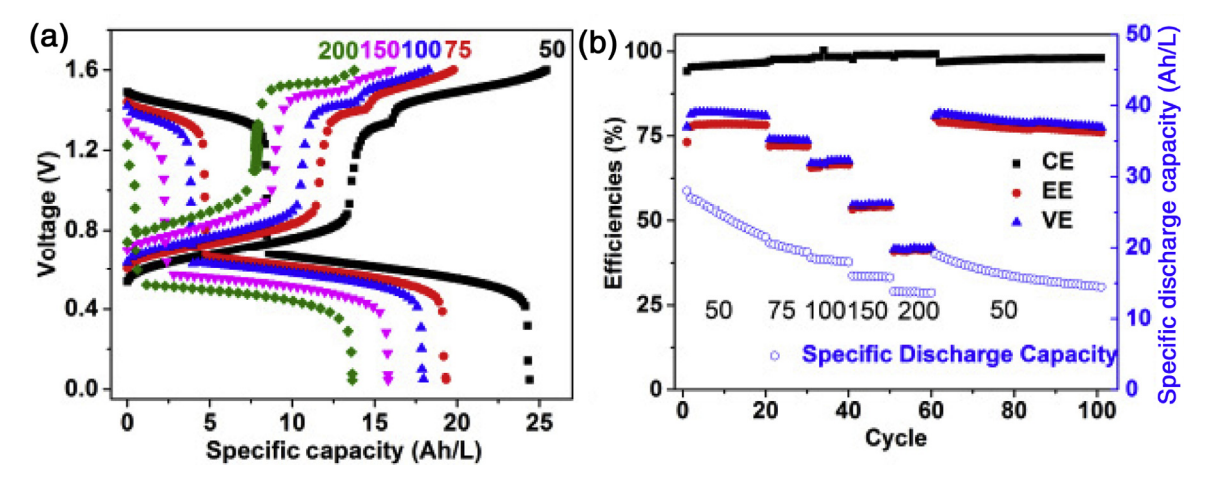


Fig. 5. Cycling performances of the V4RB cell (catholyte:anolyte volume being 2:1) with 10 mM CuCl<sub>2</sub> at the anolyte side: (a) voltage profiles at different current densities and (b) cell efficiencies and specific discharge capacities. Numbers above each voltage plot or underneath efficiency/capacity plot indicate corresponding current densities with units of mA/cm<sup>2</sup>. Voltage curves in (a) are from Cycle 10, 30, 40, 50 and 60. The theoretical volumetric capacity is 35.6 Ah/L.

laboratory operated by Battelle for DOE under Contract DE-AC05-76RL01830.

## Supplementary materials

Supplementary material associated with this article can be found, in the online version, at doi:10.1016/j.jechem.2018.05.020.

### References

- [1] Z. Yang, et al., Chem. Rev. 111 (2011) 3577-3613.
- [2] B. Dunn, H. Kamath, J.-M Tarascon, Science 334 (2011) 928-935.
- [3] M. Park, J. Ryu, W. Wang, J Cho, Nature Reviews Materials 2 (2016) 16080.
  [4] M. Skyllas-Kazacos, M. Rychcik, R.G. Robins, A.G. Fane, M.A. Green, J.Electrochem. Soc. 133 (1986) 1057–1058.
- [5] M. Skyllas-Kazacos, M.H. Chakrabarti, S.A. Hajimolana, F.S. Mjalli, M. Saleem, J. Electrochim.l Soc. 158 (2011) R55-R79.

- [6] C. Ding, H. Zhang, X. Li, T. Liu, F. Xing, J. Phys. Chem. Lett. 4 (2013) 1281-1294.
- [7] L. Li, et al., Adv Energy Mater 1 (2011) 394-400.
- [8] N. Roznyatovskaya, J. Noack, M. Fühl, K. Pinkwart, J. Tübke, J. Electrochem. Acta 211 (2016) 926–932.
- [9] O. Luo, et al., Chemsuschem 6 (2013) 268-274.
- [10] R.A. Potash, J.R. McKone, S. Conte, H.D. Abruña, J. Electrochem. Soc. 163 (2016) A338-A344.
- [11] B. Li, et al., Nano letters 13 (2013) 1330–1335. [12] L. Wei, T.S. Zhao, L. Zeng, X.L. Zhou, Y.K. Zeng, Applied Energy 180 (2016) 386-391
- [13] C.T.J. Low, C. Ponce de Leon, F.C. Walsh, Trans. of the IMF 93 (2015) 74–81.
  [14] L. Sanz, J. Palma, E. García-Quismondo, M. Anderson, J. Power Sources 224 (2013) 278-284.
- [15] B. Li, et al., Chemsuschem 7 (2014) 577–584.
  [16] W.H. Wang, X.D. Wang, Electrochimica Acta 52 (2007) 6755–6762.
- [17] W. Li, J. Liu, C. Yan, Electrochim. Acta 79 (2012) 102-108.